

The KLOE-2 experiment at DAΦNE

Paolo Gauzzi^{1,2,*} and Elena Perez del Rio^{3,**} on behalf of the KLOE-2 Collaboration

¹Dipartimento di Fisica, Università di Roma La Sapienza, P.le A.Moro 2, 00185 Rome (Italy)

²INFN - Sezione di Roma, P.le A.Moro 2, 00185 Rome (Italy)

³INFN - Laboratori Nazionali di Frascati, via E.Fermi 40, 00044 Frascati (Italy)

Abstract. The KLOE-2 Collaboration successfully ended its data-taking collecting a total integrated luminosity of 5.5 fb^{-1} at the peak of the $\phi(1020)$ resonance at the DAΦNE collider of the Frascati LNF. New detectors have been added to the KLOE apparatus to improve the detector acceptance, the tracking capability, and also to be able to tag the scattered electrons in $\gamma\gamma$ processes. By summing the new data sample to the old one of the previous KLOE data-taking ended in 2006, a total of about 8 fb^{-1} has been collected, corresponding to 24 billions of ϕ produced. The measurement program of KLOE-2 includes precision studies on kaon and other light mesons, hadronic cross-section, and dark force searches.

1 Introduction

The KLOE-2 Collaboration ended its data-taking on March 30, 2018. KLOE-2 is the continuation, with an upgraded detector, of the KLOE experiment, which collected about 2.5 fb^{-1} of data from 1999 to 2006, at the DAΦNE ϕ -factory [1] of the Laboratori Nazionali di Frascati of INFN. For this new data-taking campaign the DAΦNE collider has been upgraded with the implementation of a new interaction region based on the concept of the crab-waist collision scheme [2], which allowed to increase the machine luminosity and to reach a peak value of $2.4 \times 10^{32} \text{ cm}^{-2} \text{ s}^{-1}$ (Fig.1), and a daily integrated luminosity of 14 pb^{-1} . KLOE-2 collected a total integrated luminosity of 5.5 fb^{-1} since November 2014, at the peak of the $\phi(1020)$ resonance.

Also the KLOE detector was upgraded, new subdetectors have been inserted to improve its performances and to increase the physics reach: an Inner Tracker around the DAΦNE Interaction Point (IP) to improve tracking and vertexing, new small angle calorimeters (QCALT [3] and CCALT [4]) to increase the acceptance for low polar angle particles, and taggers for the detection of electrons and positrons scattered, associated with hadron production in interactions of virtual photons (*gammas* processes).

By adding the new data sample to the old KLOE data, a total of 8 fb^{-1} luminosity has been reached, allowing KLOE-2 to continue and to extend the KLOE physics program [5].

2 The KLOE detector

The KLOE detector consists of a large-volume Drift Chamber surrounded by a hermetic Calorimeter, both immersed in an axial magnetic field of 0.52 T produced by a superconduct-

*e-mail: paolo.gauzzi@roma1.infn.it

**Speaker, e-mail: Elena.PerezDelRio@Inf.infn.it

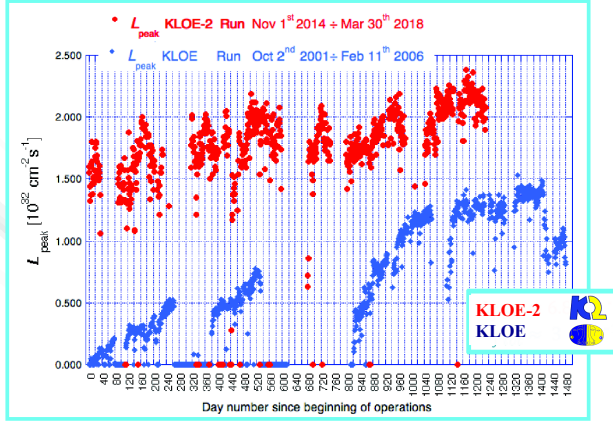


Figure 1. Comparison of the DAΦNE peak luminosity for KLOE and KLOE-2 data-taking.

ing magnet.

The Calorimeter (EMC) [6], made of Pb-scintillating fibers, was covering 98% of the solid angle, with resolutions $\sigma_E/E = 5.7\%/\sqrt{E(GeV)}$ (energy) and $\sigma_t = 55ps/\sqrt{E(GeV)} \oplus 100ps$ (time).

The Drift Chamber (DC) [7], filled with a gas mixture of He - isobutane, provided a momentum resolution $\sigma_{p_t}/p_t = 0.4\%$ for tracks emitted at large polar angles, and a space resolution of $150 \mu m$ in the plane transverse to the beam line, and 2 cm along the beam direction.

The performances of the DC and of the EMC were very stable in time, for almost 20 years since the collection of the first events, taking into account also different machine background conditions of the KLOE-2 run with respect to the KLOE one.

3 The Inner Tracker

For the KLOE-2 data-taking an Inner Tracker (IT) [8], has been installed between the beam pipe and the inner wall of the DC, 25 cm aside from the IP. It is based on the GEM technology with cylindrical geometry, and is the first detector of this kind operated in a high energy experiment. It is composed of four concentric layers of triple-GEM detectors. Each layer is made of five electrodes: the cathode, three GEM foils for electron multiplication, and the anode, acting also as readout circuit. Anodes with X-V readout have been developed for this detector: longitudinal X strips, and pads connected through internal vias to form V strips, at a stereo angle of $25^\circ \div 27^\circ$ for a total of 30000 FEE channels. The total material budget is 2% of radiation length, to minimize the multiple scattering and the photon conversion probability. Starting from tracks reconstructed in the DC, the information from the IT is added with the Kalman filter algorithm, and the track parameters are then updated. In Fig.2 the improvement in the vertical (Y) coordinate of the vertex position, which is not sensitive to beam size effects, is shown for different processes. For $\phi \rightarrow \pi^+\pi^-\pi^0$ decays the vertex resolution is $\sigma_{IT+DC} = 4.4$ mm with IT+DC compared to $\sigma_{DC} = 5.5$ mm when tracks are reconstructed with the DC only. For vertices from $K_S \rightarrow \pi^+\pi^-$ the resolution improves from $\sigma_{DC} = 10.6$ mm to $\sigma_{IT+DC} = 7.4$ mm. Further improvements are expected by using more refined alignment and calibration of the IT.

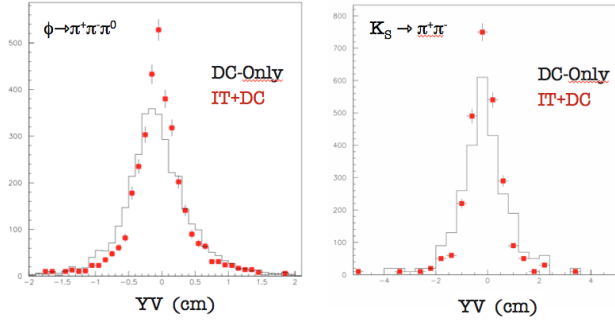


Figure 2. Y coordinate of the vertex for $\phi \rightarrow \pi^+\pi^-\pi^0$ and $K_S \rightarrow \pi^+\pi^-$ events: comparison between tracking with DC only and the integrated tracking IT + DC.

4 Taggers for $\gamma\gamma$ physics

In $\gamma\gamma$ processes, $e^+e^- \rightarrow \gamma^*\gamma^* \rightarrow e^+e^-X$, hadronic states (X) with even charge conjugation are produced. At the DAΦNE energies the single π^0 production can be accessed to measure the neutral pion radiative width ($\Gamma(\pi^0 \rightarrow \gamma\gamma)$), which has been recently remeasured with uncertainty of 1.6% by the PrimEx Collaboration [9], almost the same precision of the Chiral Perturbation Theory calculations. The Transition Form Factor (TFF) $F_{\pi^0\gamma\gamma^*}(q^2, 0)$ can also be measured at very low space-like q^2 . The TFF can be used to constrain the Hadronic Light-by-Light contribution to the theoretical calculation of the muon anomaly ($a_\mu - 2$), which is well known to be more than 3 standard deviations far from the experimental value.

Since DAΦNE is operated at the peak of the ϕ resonance, a tagging system for scattered electrons is needed to properly select the events from $\gamma\gamma$ collisions among the overwhelming background from ϕ decays. Two detectors have been installed for the KLOE-2 data-taking: the Low Energy Tagger [10], made of two LYSO crystal calorimeters readout by Silicon Photomultipliers, placed at about 1 m from the IP, and the High Energy Tagger (HET) [11], which is crucial for the detection of single π^0 's. The bending dipoles of DAΦNE act as spectrometers for the scattered electrons and positrons resulting in a strong correlation between the particle energy and its trajectory, thus the HET consists of two scintillator hodoscopes readout by standard PMTs placed 11 m far from the IP, inserted in roman pots close to the beam line (see Fig.3). The counting rate of the taggers is largely dominated by Bhabha scattering. The analysis of the events in which either a single HET station is hit (Single Arm) or both HET stations are in coincidence (Double Arm) is in progress. MultiVariate Analysis (MVA) is exploited to separate signal from the Bhabha background; the $e^+e^- \rightarrow e^+e^-\pi^0$ events are simulated by the Ekhara 2.1 Monte Carlo (MC)[12].

5 Kaon physics at KLOE

At a ϕ -factory neutral and charged kaons are produced in an antisymmetric state with quantum numbers $J^{PC} = 1^{--}$. For neutral kaons this implies that the presence of a K_S (K_L) on one

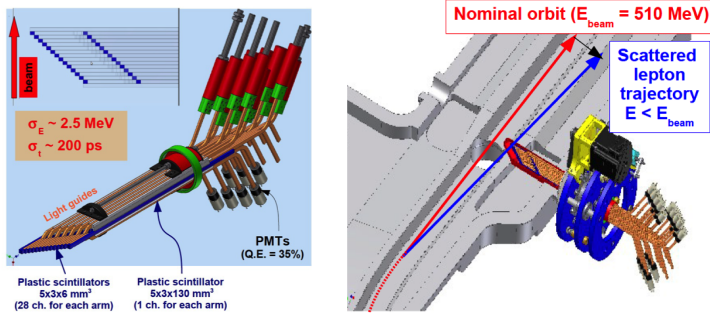


Figure 3. Scheme of a HET station: scintillator hodoscope (left); positioning in the DAΦNE beam-pipe (right).

side of the detector can be used to tag the presence of K_L (K_S) on the other side, with opposite momentum. The ϕ -factory thus provides a unique possibility to select a pure K_S beam, contrary to the fixed-target experiments. The entanglement and the interference pattern of the decay of the kaons allow for precision studies of the fundamental symmetries of nature and several tests of quantum mechanics (see also ref. [13]).

K_S charge asymmetry

For semileptonic decays of neutral kaons, the charge asymmetries can be measured:

$$A_{S,L} = \frac{\Gamma(K_{S,L} \rightarrow \pi^- e^+ \nu) - \Gamma(K_{S,L} \rightarrow \pi^+ e^- \bar{\nu})}{\Gamma(K_{S,L} \rightarrow \pi^- e^+ \nu) + \Gamma(K_{S,L} \rightarrow \pi^+ e^- \bar{\nu})} \quad (1)$$

Both asymmetries are expected to be different from zero, due to CP violation. For the K_L case the asymmetry was precisely measured by the KTeV Collaboration and was found to be $A_L = (3.322 \pm 0.058 \pm 0.047) \times 10^{-3}$. Any significant difference between A_S and A_L would be a clear signal of CPT violation.

The whole sample collected during the first KLOE data-taking has been analyzed, corresponding to 1.7 fb^{-1} of integrated luminosity, about 4 times the statistics of the previous KLOE measurement of the same quantity. In Fig.4 the lepton invariant masses are shown in comparison with the MC simulation.

The new result is $A_S = (-4.9 \pm 5.7 \pm 2.6) \times 10^{-3}$, and the combination with the old KLOE value gives $A_S = (-3.8 \pm 5.0 \pm 2.6) \times 10^{-3}$ [14]. From the analysis of the whole KLOE-2 statistics, together with the improved tracking, the statistical uncertainty is expected to be reduced at the level of 3×10^{-3} .

$K_{S\ell 3}$ decays

The K_{Se3} semileptonic decay gives also the largest contribution to the uncertainty on the V_{us} element of the CKM matrix. The whole KLOE data sample is being analyzed in order to reduce this uncertainty.

The measurement of the $K_{S\mu 3}$ decay is a test of lepton universality, and moreover, this branching fraction has never been measured up to now. The preliminary distribution of the squared invariant masses of the leptons (in the muon hypothesis) is shown in Fig.5. The evaluation of the systematic uncertainty on the branching fraction is in progress.

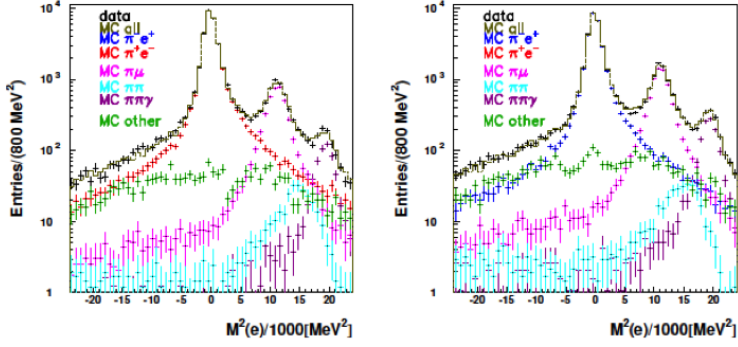


Figure 4. Lepton mass squared (in the electron/positron hypothesis) for the two different charges in semileptonic K_S decays.

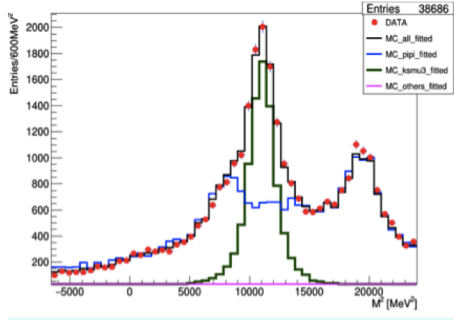


Figure 5. Invariant mass squared the lepton (in the muon hypothesis) in $K_S\mu_3$ semileptonic decays.

$$K_S \rightarrow 3\pi^0$$

The $K_S \rightarrow 3\pi^0$ decay is purely CP violating, and also this decay has been never observed before. The SM prediction for the branching fraction can be obtained from the CP violation parameters from K_L decays, and is about 2×10^{-9} . The best upper limit, $Br(K_S \rightarrow 3\pi^0) < 2.6 \times 10^{-8}$ at 90% C.L. was determined by KLOE with 1.7 fb^{-1} of data.

To improve the upper limit the search for this decay with the new KLOE-2 data has started. By exploiting the full KLOE-2 statistics and optimizing background reduction, it will be possible to reach a sensitivity of the order of 10^{-8} for the branching fraction.

6 Measurement of the running of the fine-structure constant

The fine-structure constant α_{em} is a running parameter due to vacuum polarization effects, $\alpha_{em}(s) = \frac{\alpha_{em}(0)}{1 - \Delta\alpha}$. The value of $\alpha_{em}(s)$ can be extracted from the ratio of the differential cross-section of $e^+e^- \rightarrow \mu^+\mu^-\gamma$ with an Initial State Radiation (ISR) photon, to the corresponding cross-section with $\alpha_{em} = \alpha_{em}(0)$ obtained from a MC simulation; s is the momentum transfer

squared of the reaction.

$$\left| \frac{\alpha_{em}(s)}{\alpha_{em}(0)} \right|^2 = \frac{d\sigma_{ISR}(e^+e^- \rightarrow \mu^+\mu^-\gamma(\gamma))/d\sqrt{s}}{d\sigma_{MC}^0(e^+e^- \rightarrow \mu^+\mu^-\gamma(\gamma))/d\sqrt{s}} \quad (2)$$

Two charged tracks at large angle are selected, while the ISR photon is required to be at small angle, inside the beam-pipe. The photon is not detected and its momentum is reconstructed from the kinematics of the events. The ratio of eq.(2) is shown in Fig.6 in comparison with the theoretical prediction based on dispersion relations [15].

$\Delta\alpha$ is a complex parameter in the time-like region. From the optical theorem follows that $\Im(\Delta\alpha) = -\frac{\alpha}{3}R(s)$, and it has been obtained from the KLOE measurements of the hadronic cross-section. Then the real part of $\Delta\alpha$ (Fig.6) is determined:

$$\Re(\Delta\alpha) = \sqrt{\left| \frac{\alpha_{em}(s)}{\alpha_{em}(0)} \right|^2 - [\Im(\Delta\alpha)]^2} \quad (3)$$

The result of the measurement shows that there is a clear contribution of the ρ and ω resonances to the photon propagator. Additionally, from a fit to the $\rho - \omega$ interference pattern the $Br(\omega \rightarrow \mu^+\mu^-) = (6.6 \pm 1.4 \pm 1.7) \times 10^{-5}$ has been evaluated [16].

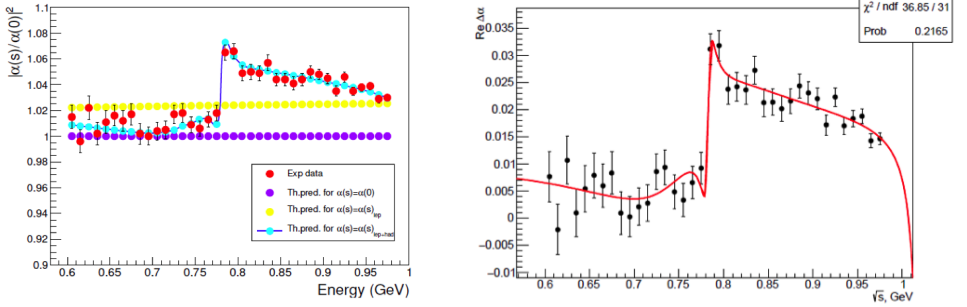


Figure 6. Running of α_{em} (left), and $\Re(\Delta\alpha)$ (right), showing the $\rho - \omega$ contribution to the photon propagator.

7 η rare decays

$\phi \rightarrow \eta\gamma$ has a branching fraction of $\approx 1.3\%$, thus a large amount of η mesons is produced at a ϕ -factory and it can be used to study rare decays of this meson.

The decay $\eta \rightarrow \pi^0\gamma\gamma$ is a golden mode of Chiral Perturbation Theory, as it is sensitive to $O(p^6)$ terms, being $O(p^2)$ null for neutral mesons, and $O(p^4)$ suppressed by G -parity. The PDG $Br(\eta \rightarrow \pi^0\gamma\gamma) = (25.6 \pm 2.2) \times 10^{-5}$ comes from the Crystal Ball measurements [17, 18], while there is an old preliminary KLOE measurement significantly lower, $Br(\eta \rightarrow \pi^0\gamma\gamma) = (8.4 \pm 3.0) \times 10^{-5}$. This decay is characterized by 5 prompt photons in the final state. The dominant background comes from $\eta \rightarrow 3\pi^0$ with either lost or merged photons, and MVA methods are currently exploited to disentangle the real 5 photon events from the background.

The decay $\eta \rightarrow \pi^+\pi^-$ violates both P and CP symmetries. The branching fraction according to the SM is expected of the order of 10^{-27} , the detection at any accessible level would be a signal of P and CP violation from other sources beyond the SM [19]. The best limit was previously obtained by KLOE, with 350 pb^{-1} of data, $Br(\eta \rightarrow \pi^+\pi^-) < 1.3 \times 10^{-5}$ at 90% C.L. [20]. In Fig.7 the distributions of the mass of the charged tracks and the invariant mass of the two charged tracks in the event are compared with the MC simulation. A preliminary upper limit can be set from the invariant mass distribution in the region of the η mass, $Br(\eta \rightarrow \pi^+\pi^-) < 5.8 \times 10^{-6}$ at 90% C.L. [12]). By combining the old KLOE data with the new KLOE-2 sample, the limit is expected to decrease by a factor of about two.

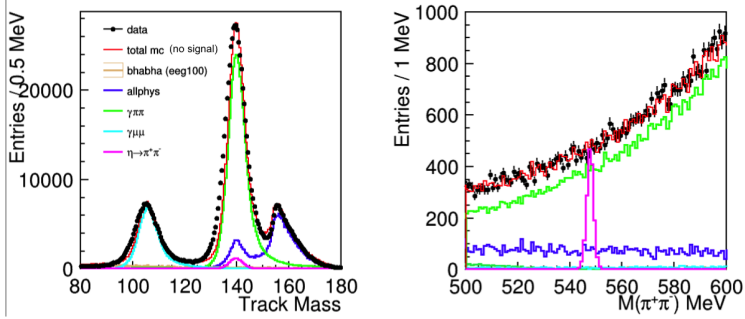


Figure 7. Left: distribution of the mass of the charged tracks; Right: two track invariant mass in the region of the η mass, the peak of $\eta \rightarrow \pi^+\pi^-$ has been generated by MC with an arbitrary branching fraction.

8 Dark Matter searches

The existence of particles belonging to a dark sector has been proposed to explain many astrophysical observations and other anomalies. Extensions of the SM predict the presence of an additional gauge symmetry associated to a light vector boson, *dark photon*, that couples through kinetic mixing to particles of the Standard Model (SM).

The dark photon (U) can be produced in process like $e^+e^- \rightarrow U\gamma$. A ϕ -factory is a suitable facility for these studies, since the cross-section scales as $1/s$, being about 100 times greater than at the B-factories and compensating for the lower integrated luminosity. A summary of the KLOE searches of the dark photon can be found in ref. [21].

The signature of the (invisible) decay of the dark photon into dark matter particles would be a single monochromatic photon. During the second part of the KLOE-2 data-taking a new Single Photon Trigger (SPT) has been implemented, by requiring an energy deposit of at least $E > 350 \text{ MeV}$ in the barrel part of the EMC. This trigger can also be useful to search for another kind of exotics, the Axion Like Particles (ALPs) [22]. If a long living ALP is produced in $e^+e^- \rightarrow \gamma^* \rightarrow a\gamma$, the signature will also be a single monochromatic photon. A total luminosity of 2.7 fb^{-1} of data has been collected with the SPT, allowing to explore the region of masses below 600 MeV.

With the KLOE data a search of another kind of dark force mediator, a leptophobic boson (B -boson) mainly coupled to quarks [23] is in progress. The dominant decay channel for masses below 600 MeV, is $B \rightarrow \pi^0\gamma$. Then, the $\phi \rightarrow \eta B \rightarrow \eta\pi^0\gamma$ and $\eta \rightarrow B\gamma \rightarrow \pi^0\gamma\gamma$ decay chains can be exploited looking for possible peaks in the $\pi^0\gamma$ invariant mass in the 5 prompt photon final state sample [21].

9 Conclusions

A unique worldwide sample of data has been collected by the KLOE/KLOE-2 Collaboration at the DAΦNE ϕ -factory of the LNF in Frascati in two data-taking campaigns, the first from 1999 to 2006, and the second from November 2014 to March 2018. A total luminosity of 8 fb^{-1} has been collected, corresponding to about $24 \times 10^9 \phi$ mesons produced.

Along the years, the Collaboration has produced relevant results on the discrete symmetries of nature, on the decay dynamics of light mesons, on the hadronic cross-section via the ISR method, on transition form factors, and also on the search for New Physics in the dark sector. With the new sample collected with the upgraded detector, the high precision investigation of light hadron physics and of fundamental symmetries will continue in the next years.

References

- [1] A. Gallo et al., Conf. Proc. **C060626**, 604 (2006)
- [2] M. Zobov et al., Phys. Rev. Lett. **104**, 174801 (2010)
- [3] M. Cordelli et al., *QCALT: A tile calorimeter for KLOE-2 experiment*, in *Astroparticle, particle and space physics, detectors and medical physics applications. Proceedings, 11th International Conference on Advanced Technology and Particle Physics, ICATPP 11, Como, Italy, October 5-9, 2009* (2009), pp. 404–408
- [4] F. Happacher, M. Martini, S. Miscetti, I. Sarra, Nucl. Phys. Proc. Suppl. **197**, 215 (2009), [0906.1157](#)
- [5] G. Amelino-Camelia et al., Eur. Phys. J. **C68**, 619 (2010), [1003.3868](#)
- [6] M. Adinolfi et al., Nucl. Instrum. Meth. **A482**, 364 (2002)
- [7] M. Adinolfi et al., Nucl. Instrum. Meth. **A488**, 51 (2002)
- [8] A. Balla et al., Nucl. Instrum. Meth. **A845**, 266 (2017)
- [9] I. Larin, these proceedings (2019)
- [10] D. Babusci et al., Nucl. Instrum. Meth. **A617**, 81 (2010), [0906.0875](#)
- [11] F. Archilli et al., Nucl. Instrum. Meth. **A617**, 266 (2010)
- [12] F. Curciarello, these proceedings (2019)
- [13] A. Di Cicco, these proceedings (2019)
- [14] A. Anastasi et al. (KLOE-2), JHEP **09**, 021 (2018), [1806.08654](#)
- [15] F. Jegerlehner, Nuovo Cim. **C034S1**, 31 (2011), [1107.4683](#)
- [16] A. Anastasi et al. (KLOE-2), Phys. Lett. **B767**, 485 (2017), [1609.06631](#)
- [17] S. Prakhov et al., Phys. Rev. **C78**, 015206 (2008)
- [18] B.M.K. Nefkens et al. (A2 at MAMI), Phys. Rev. **C90**, 025206 (2014), [1405.4904](#)
- [19] C. Jarlskog, E. Shabalin, Phys. Scripta **T99**, 23 (2002)
- [20] F. Ambrosino et al. (KLOE), Phys. Lett. **B606**, 276 (2005), [hep-ex/0411030](#)
- [21] E. Perez del Rio, these proceedings (2019)
- [22] W.J. Marciano, A. Masiero, P. Paradisi, M. Passera, Phys. Rev. **D94**, 115033 (2016), [1607.01022](#)
- [23] S. Tulin, Phys. Rev. **D89**, 114008 (2014), [1404.4370](#)